Microstructural Characterization and Wear Behavior of Porous Equimolar TiNbZr Medium-Entropy Alloys Scaffolds Produced by Mechanical Alloying

Şükran Karadeniz[a]* 🆔 *, Ersin Arslan[b]*

[a]*Ataturk University, Department of Metallurgical and Materials Engineering, 25240, Erzurum, Turkey.*
[b]*Istanbul Aydin University, Department of Mechanical Engineering, 34295, Istanbul, Turkey.*

Recently, there has been increasing importance on scaffold materials that could be used in biomaterials. In the present study, equimolar TiNbZr medium entropy alloys (MEAs) and porous TiNbZr alloy scaffolds were produced by mechanical alloying (MA) that is a powder metallurgy processing technique. The MA process was carried out using high energy planetary ball mill. Ammonium bicarbonate (NH_4HCO_3) at different percentage ratio was used as space holder to fabricate the porous TiNbZr scaffolds with using space-holder sintering method. Cold Isostatic Pressing (CIP) was performed for consolidation of mechanically alloyed powders. Finally, the green compact samples were sintered in tube furnace under vacuum atmosphere. The microstructural analyses, phase composition, porosity and density measurement, compression and microhardness tests and wear resistance of bulk alloys were examined. The X-Ray Diffraction (XRD) patterns of all samples indicated the dominant β-Ti phases and small amount of α-Ti phase. SEM (scanning electron microscope) images for porous TiNbZr alloy scaffolds demonstrated that porosity increased with increase of space holders amount. With the increasing porosity content, density, hardness, compressive strength and the elastic modulus of samples decreased while wear rate increased.

Keywords: *Equimolar TiNbZr alloy, Medium-entropy alloys, Porous scaffolds, Powder metallurgy, Mechanical property, Wear behavior, Cold isostatic press, Space-holder method, Ammoniumhydrogen carbonate (NH_4HCO_3).*

1. Introduction

Metals and their alloys have been commonly used in the field of human implants and organ repair for many years because of the their high strength, good corrosion resistance and biocompatibility. The metal biomedical materials which was used in commercial mainly include Co-Cr alloys, stainless steels, titanium (Ti) and Ti alloys[1]. Ti and its alloys exhibit exceptional mechanical and physical properties like a high strength to weight ratio, low density, perfect corrosion resistance, so they are preferred in the field of biomaterials[2]. Additionally, currently used Ti and its alloys e.g. Ti-6Al-7Nb, Ti-5Al-2.5Fe (wt.% hereafter) and Ti-6Al-4V are tend to release toxic aluminum (Al) or vanadium (V) ions day after day later implant surgery. So they can reason for Alzheimer's disease and mental problems[3]. In addition, these alloys and pure Ti (110 GPa) show considerably higher Young's modulus than that of a human bone (30 GPa). For biomaterials, elastic modulus is the most important property[4]. Stress shielding, bone resorption, and poor osseointegration may occur due to mismatch between the elastic modules of implants and bone tissue[5-8]. So, developmental research is needed to new Ti alloys with nontoxic alloying elements which is suitable properties for biomaterials. For example, elements like Molybdenum (Mo), niobium (Nb), tantalum (Ta), zirconium (Zr) and have low elastic modulus, excellent strength and biocompatibility, which are necessary for biomedicine[9].

Medium entropy alloys (MEAs) have been intensively researched in recent years and have become a new type of advanced metal structural and functional materials. MEAs usually compose of multiple elements mixed in an equimolar or nearly equimolar ratio, and have a simple microstructure with the solid-solution phase due to the high configurational entropy effect, but may give an attractive balance of mechanical properties[10,11]. Recent times, for usage as biomaterials, MEAs have been reported to exhibit great potential[12,13]. The Ti-Nb-Zr alloy has attracted great research interests between the alls[14,15]. Nowadays, MEAs consisting of Ti, Nb and Zr elements, attract great attention. Nb and Zr addition enhances both the mechanical properties and corrosion and wear resistance of the material and their use in low modulus β or α/β Ti implant materials increases[16,17].

So, a new β-type equimolar TiNbZr alloy has been produced by PM method. As a result of the analyzes it was observed that low elastic modulus (84 GPa) and high compressive strength (1155 MPa). However, the difference in elastic modulus of natural bone with bulk equimolar TiNbZr alloy was still found to be large, hence a new material was needed. It is known that the porosity of the materials reduces the elastic modulus and thus the compatibility with the modulus of elasticity of the bone increases. In this way, stress shielding is also prevented[18]. With porous structure, both strong bonding could be actualized between the implants and natural bone and cellular activity like cell migration[19,20]. Moreover, open

*e-mail: gurcansukran@gmail.com

porous and interconnected networks in the porous structure play an important role for cell nutrition and waste removal. Until now, the PM space holder, additive manufacturing (AM) and foaming techniques are the most well-known methods for the production of porous scaffolds[21-23]. Between them, PM space-holder technique has more advantages to control over pore fraction and shape and also this technique is more suitable and economic. Sodium chloride (NaCl), ammoniumhydrogen carbonate (NH_4HCO_3), carbamide (CH_4N_2O), saccharose sugar pellets, magnesium powder and tapioca are mostly using space-holder materials[24]. Between all space-holder materials NH_4HCO_3 can be easily removed by sintering during scaffold fabrication and is cheap so it is most suited for fabricating porous Ti scaffolds.

In the present study, firstly equimolar TiNbZr alloy was produced by PM. This alloy has not been encountered before in the literature. After that, equimolar TiNbZr alloy scaffolds were fabricated by PM using NH_4HCO_3 as the space-holder material. Sodium chloride, ammoniumhydrogen carbonate, carbamide, saccharose sugar pellets, magnesium powder and tapioca could be used as space-holder. Among them, NH_4HCO_3 is considered a good potential due to low cost and easy removal that results in good shape retention. At the same time, the production of porous equimolar TiNbZr alloy scaffolds by PM space holder method represents a first and there has been no study for porosity, density, mechanical and wear properties of this manufactured scaffolds. The mechanical properties, phase composition and structure of the equimolar TiNbZr alloy and porous equimolar TiNbZr alloy scaffolds were analyzed using SEM, EDS (energy dispersive X-ray spectrometer), XRD, pin-on-disc wear test and compression tests. And also Archimedes' method were applied to measure the densities of the all samples.

2. Materials and Methods

2.1. Specimen preparation

In the presented study, equimolar TiNbZr alloy was synthesized by MA and powder metallurgical process. The elemental metal powders of Ti (purity: 99.9 wt%, particle size: 45μ), Nb (purity: 99.9 wt%, particle size: 45μ) and Zr (purity: 99.9 wt%, particle size:45μ) were used as initial materials. In order to prevent extensive oxidation of milled powder, the jar was loaded and unloaded in high-purity argon atmosphere in glove box. Ti, Nb and Zr were prepared equiatomic fraction for using MA method (33Ti33Nb33Zr). In powder mixing process the atomic ratios of the elements (33Ti33Nb33Zr) were converted into mass ratios was the first step. MA was carried out using Retsch PM 100 planetary ball mill with rotation speed 300 rpm with tungsten carbide jar and balls. The ball-to-power weight ratio of 10:1 was selected and time of alloying was 30 h. 1% wt. stearic acid was added as a process control agent.

The as-milled equimolar TiNbZr powder and space-holder particles (NH_4HCO_3) were blended with planetery ball milling for 3 h. Ball to powder weight ratio of 3:1 was selected for blending. After mixing process, the mixture powders were cold-pressed at 300 MPa and the green compacts were sintered in two steps. A high vacuum furnace was used for all sintering process. In the first step samples were heated at 180 °C for 2 h to burn out the NH_4HCO_3 particles. In the second step sintering was completed in a high vacuum of about 10^{-5} torr. at 1500° C for 2 h.

Cylindrical samples with a length of 20 mm were prepared for analyzing the elastic modulus and compressive strength, while disc samples with a length of 2 mm were prepared for other tests. All samples were 13 mm diameter.

Porous TiNbZr alloys with porosities fabricated by adding 20, 30 wt. % space holder (S.H.) to the powder mixture are shown in Table 1.

2.2. Materials characterization

The porosity and density were analyzed based on the Archimedes method.

The compression test was carried out using a compression testing machine (Instron) at room temperature at the strain rate of 0,5 mm/min. The engineering stress strain curves were used for calculating the compressive yield strength and elastic modulus of samples. Microhardness of samples were measured using the Vickers indenters. (HMV-G Shimadzu),

The microstrucures of specimens were showed using FEI-INSPECT S50 Scanning Electron Microscope (SEM) respectively. The phase composition of fabricated samples were analyzed with a scanning electron microscope equipped with EDS. For micro hardness and SEM investigations specimens were prepared using standard metallographic techniques. Sample's surfaces were prepared by grinding, polishing and etching.

The crystal structures of the samples were analyzed by using an Bruker D2 Phaser X-Ray diffraction (XRD) instrument with Cu-Kα irradiation as photon source (λ= 1.5406 A˚) in 2θ ranges between 20º and 100°.

Wear tests were performed on a Tribotechnic pin-on-disc tribometer in dry conditions and with the uniform environmental conditions. The main optimized parameters of wear test; A 6-mm diameter tungsten carbide (WC) ball 4N load, 20 mm/s speed and test distance of 50 m. In addition, the wear scars examined by SEM and the WC balls examined by optic microscope to analyze the effects of the wear mechanisms involved in the process.

3. Results and Discussion

The XRD patterns of equimolar TiNbZr alloy and porous TiNbZr alloy scaffolds with different NH_4HCO_3 (Space holder S.H.) weight ratios were shown in Figure 1 (JCPDS No. 00-044-1288). It was clear that the NH_4HCO_3 had no apparent effect on the XRD patterns of the equimolar TiNbZr scaffolds. The diffraction peaks showed that the equimolar TiNbZr alloy scaffolds were consisted of two different phases called α-Ti and β-Ti. However, when the main peak intensities of the two phases were compared, the amount of

Table 1. Mixing ratio for TiNbZr powder and space holder.

Mixture	TiNbZr (wt. %)	NH_4HCO_3 (wt. %)
I	100	-
II	80	20
III	70	30

α phase was lower than beta. After MA the diffraction peaks of Nb and Zr elements disappeared.

The compressive strength and elastic modulus of cylindrical equimolar TiNbZr alloys and porous TiNbZr samples were analyzed using the compression testing method. Results were listed in Table 2. The elastic modulus and compressive strengths of the equimolar TiNbZr alloy were 84 GPa and 1155 MPa. As seen in Table 2, the elastic modulus and compressive strengths of the as-fabricated porous alloys decreased with an increase NH_4HCO_3 content, and ranges from 52 GPa to 15 GPa and 981 MPa to 124 MPa, that was as close as possible elastic modulus of the natural bone. As it is known, the porosity, the phase and grain size in the microstructure of the alloy play a major role in the change of strength. When the sample porosity increase, strength decrease. Moreover, the properties of the moderate and high porosity structure in alloys showed a high level of compatibility with cortical bone (compressive strength: 114–195 MPa and elastic modulus: 10–30 GPa)[25]. When the mechanical test results were evaluated, since the scaffold production of equimolar TiNbZr alloy scaffolds eliminates the mechanical incompatibility between the implant material and the bone, it was predicted that it will minimize the risk of instability and prevent early implant loosening.

In order to determine the mechanical properties of the obtained alloys, microhardness measurements were applied. Vickers microhardness measurements were performed to determine the differences in microhardness with increasing NH_4HCO_3 content in alloys. The Vickers hardness of each alloy is listed in Table 2. Equimolar TiNbZr exhibited the highest hardness (1100 HV) while the samples which contain 30% NH_4HCO_3 showed the lowest hardness (475 HV). It was

Figure 1. X-ray diffraction patterns of the equimolar TiNbZr alloys with different weight ratios of NH_4HCO_3 (S.H.) added: a) Equimolar TiNbZr; b) 20 wt% NH_4HCO_3: 80 wt% TiNbZr; c) 30 wt% NH_4HCO_3: 70 wt% TiNbZr.

observed that, when the porosity of sample is increased, microhardness value is decreased. Also all hardness values were higher than the cp- Ti hardness (286 HV) because increase the amount of β phase which is harder than α phase and consequently, hardness value also increased[26]. The hardness are also higher than some recently developed biomedical TiNbZr alloys such as Ti-13Nb-13Zr, Ti-24Nb-4Zr[27,28].

Measured density and calculated porosity of the equimolar TiNbZr alloy and equimolar TiNbZr scaffolds in cold pressed and 1500°C sintering temperature are shown in Table 2. the equimolar TiNbZr density was 6.4 g/cm³ and its porosity was close to 0.5%. It can be noticed that, with increasing the NH_4HCO_3 ratio from 20% to 30%, the porosity increased from 31,7% to 49,4% and density decreased from 3,5 (gr/cm3) to 2,9 (gr/cm3) respectively. The pore properties and density of the scaffold are the properties that determine the use of a scaffold as an implant material. The porosity of the implant material is between about 30-90%, allowing new bone tissues to grow within the material. So, the porosity values of the produced these scaffold materials were suitable for the development of new bone tissues. And also with the addition of 20% and 30% (wt.) NH_4HCO_3, the average pore size of porous TiNbZr scaffolds was observed from 220 μm to 550 μm, which is in the desired pore size range for bone tissue growth."
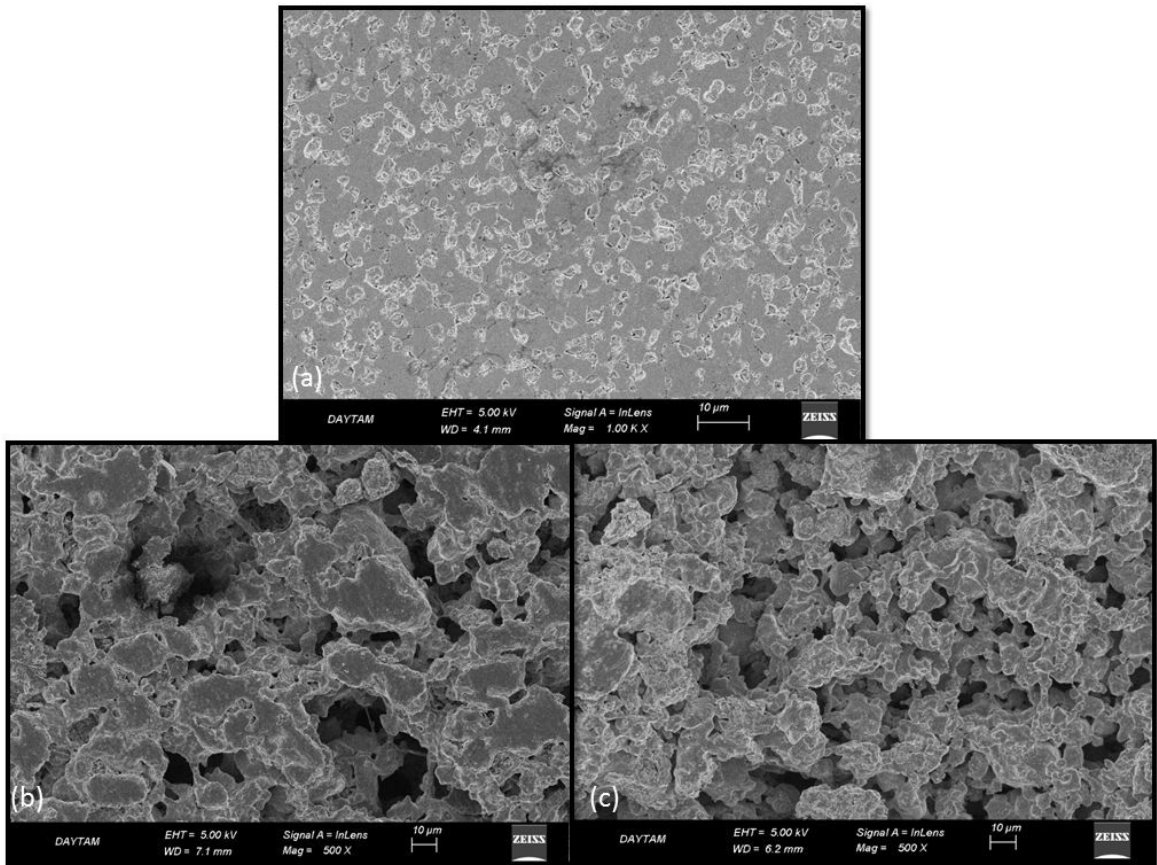
SEM images of the equimolar TiNbZr alloy and porous TiNbZr alloys with different the NH_4HCO_3 added are shown in Figure 2. The equimolar TiNbZr alloy has presented high densification after sintering, with homogeneous microstructure. The dissolution of Nb particles directly affects the microstructural development of the P/M equimolar TiNbZr alloy[29]. In high temperature Nb cores disolve and there is the stabilization of a wide phase area. In Figure 2a, it was observed that the Nb and Zr particles were dissolved during sintering (1500°C). According to detailed EDS analysis the atomic composition of the designed TiNbZr alloys was Ti-33.31 at.%Nb-33.02 at.%Zr, which are consistent with the nominal composition of each alloy. Two phases are seen in scanning electron microscope images; one of them is β-phase which is seen as light grey and the other one is α-phase seen as dark grey. EDS analysis confirmed that the Nb is present in larger amount in β-areas and a higher Ti concentration is present in α-plates. The atomic composition of the light grey area seen as Figure 2 was Ti-77.45 at.%Nb, 10.24 at.% Zr which is corresponding to β-phase. The atomic composition of dark grey area seen in the microstructure of sample was Ti- 10.52 at.%Nb-15.55 at.%Zr, which is corresponding to α-phase. Absolute dissolution of alloying elements in the Ti matrix (~1500 ºC) is the desired combination of mechanical and physical properties. It can be seen from Figure 2b-2c, with an increase in NH_4HCO_3 ratio from 20% to 30%, the
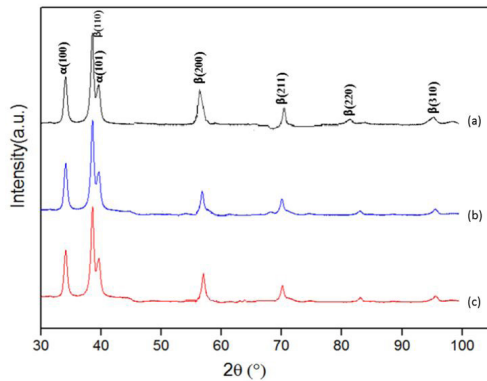
Table 2. Density, porosity, mechanical properties and wear rate of specimens of equimolar TiNbZr alloy and porous equimolar TiNbZr with different porosities.

Specimen	Density (gr/cm³)	Porosity (%)	Hardness (HV)	Elastic Modulus (GPa)	Compressive Strenght (MPa)	COF	Wear Rate (mm³/N/m)
Equimolar TiNbZr	6.4	0.5	1100	84	1155	0.14	4.0055 E⁻⁶
20% S.H.	3.5	31.7	765	52	981	0.17	2.6680 E⁻⁴
30% S.H.	2.9	49.4	475	15	124	0.19	3.7783 E⁻⁴

Figure 2. SEM images of the equimolar TiNbZr alloys with different weight ratios of NH_4HCO_3 added: a) Equimolar TiNbZr; b) 20 wt% NH_4HCO_3: 80 wt% TiNbZr; c) 30 wt% NH_4HCO_3: 70 wt% TiNbZr.

pore size increased gradually. The porosity of the consisting porous TiNbZr alloy can be changed by adjusting the amount of space-holder particles[30]. Additionally, because of the two different type of irregular shapes (micro pores and macro pores) the pores of the porous structures were not regular distributed. Volumetric shrinkage during sintering probably created micropores of micrometer size, while the macro pores were caused by the vaporization of NH_4HCO_3. The macro pores increased remarkably with increasing the NH_4HCO_3 content. It is mostly believed that the combination of micro pores and macro pores in the scaffold can improve the efficiency of new bone regeneration and so enhancing osseointegration[31].

The production of high wear resistant alloy is difficult. The substance properties such as hardness and strength have playing an essential role in wear[32]. Coefficient of friction (COF) and wear rate of the samples were shown in Table 2. A slight increase in the COF value with porosity was observed (Figure 3). Also it seems that the friction coefficients have direct corresponding relation with wear. It was observed that the wear rates increased with as the amount of NH_4HCO_3 in the samples so samples which contain 30% NH_4HCO_3 presented more damages at the surface with wide wear scar. Additionally there is a relationship between wear rate and hardness. Wear rate were decreased with increase of hardness of the alloy[33]. When equimolar TiNbZr was analyzed, the continuity and
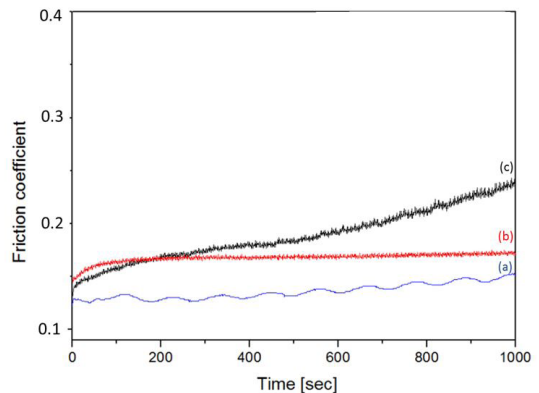
Figure 3. Evolution of friction coefficient versus time equimolar TiNbZr alloys with different weight ratios of NH_4HCO_3 added: a) Equimolar TiNbZr; b) 20 wt% NH_4HCO_3: 80 wt% TiNbZr; c) 30 wt% NH_4HCO_3: 70 wt% TiNbZr.

width of the abrasion marks do not indicate extensive wear and material loss. It was seen that an abrasive type of wear mechanism is formed due to the scratches on the surfaces of the parts broken off from the sample surfaces during the abrasion test. In addition, it was observed that some particles detached from the sample during plastic deformation during wear remain between the sample and the disc and adhere

to the surface again with the help of the heat generated as a result of friction. Therefore, it can be said that both abrasive and adhesive wear mechanisms occur for the surface damage observed on the wear surfaces. With being of third bodies can change two body to three body wear mechanism. In all situation with along wear tests, material transfer which

characterizes the adhesion phenomena was seen under naked eyes from the equimolar TiNbZr alloy to ball. (Figure 4). SEM images of worn surfaces were showed in (Figures 4-5). As seen in Figures 4-5, all porous samples had same wear mechanisms. Gradual removal or deformation of material on solid surfaces with abrasive wear on specimens. Damage
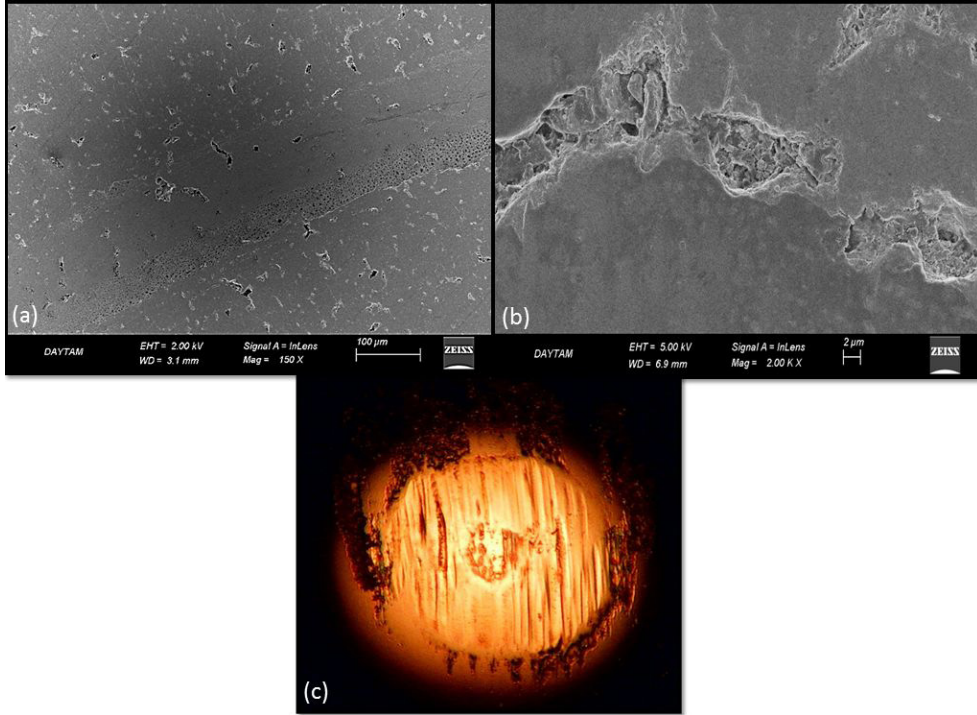

Figure 4. SEM images of the wear scar of samples a,b) equimolar TiNbZr alloy; c) counter-material surfaces.
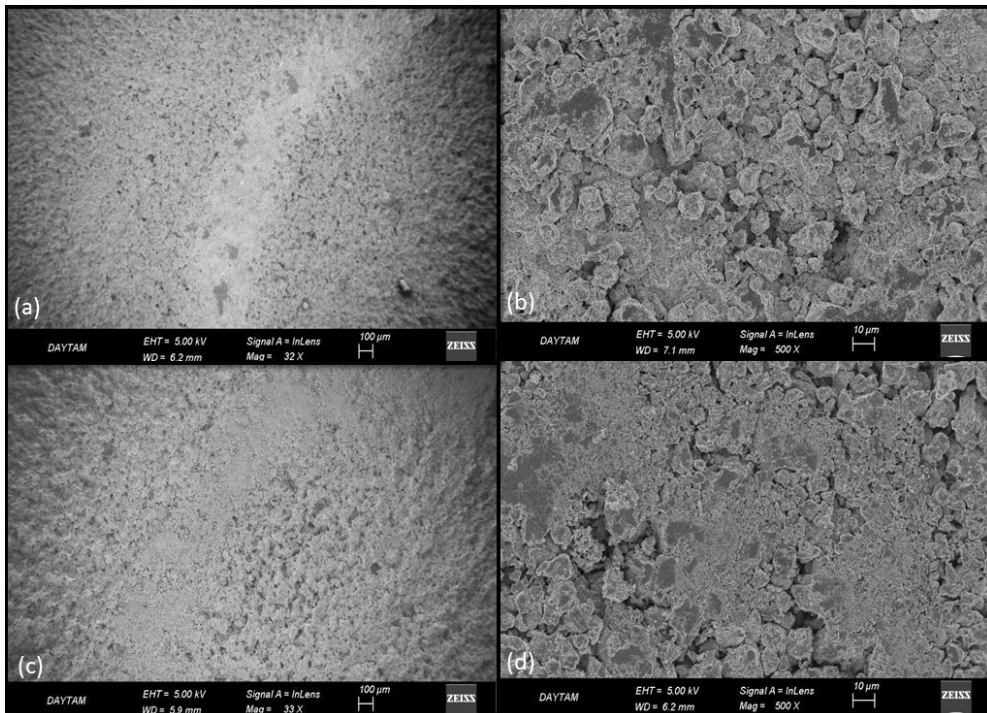

Figure 5. SEM images of the wear scar of samples a,b) 20 wt% NH_4HCO_3: 80 wt% TiNbZr; c,d) 30 wt% NH_4HCO_3: 70 wt% TiNbZr.

in the form of grooves caused by abrasive particles was observed in wear scar surface. When the wear trace was examined, shallow wear tracks with parallel micro grooves running in the sliding direction and filler particles put out were analysed. Also, the deep ploughing grooves, ridges and chips observed. The presence of pores effect on the wear behaviour of materials. It can be seen from the Figures that the wear rate increases with increasing porosity of samples. However, pores decrease the real area of contact between two sliding surfaces and therefore increase the contact pressure. Pores in the samples are a kind of serious microstructure defect. Porosity affects wear properties by softening the material and also increasing subsurface cracking and delamination[34].

4. Conclusions

Porous equimolar TiNbZr alloy scaffolds were fabricated via powder metallurgy through adding NH_4HCO_3. The XRD diffraction peaks denoted that the equimolar TiNbZr scaffolds were consisted of two phases (major β-Ti phase and minor α-Ti phase). However, when the main peak intensities of the two phases were compared, it was observed that the amount of the α phase was much lower than the β phase. Porosity, density, microstructure, elastic modulus, compressive strength, hardness and wear behaviour were investigated. By adjusting the mass ratio of the NH_4HCO_3, the porosity of the fabricated porous scaffolds could be controlled in the range 31,7- 49,4%. The compressive strengths, elastic modulus and hardness of the samples decrease with increasing porosity, as expected too. And also the alloy with high porosity has a visibly larger wear rate fluctuation than the alloy with low porosity. This porous equimolar TiNbZr scaffold fabricated by PM is a encouraging new implant material for especially bone-tissue engineering.

5. References

1. Yuan Y, Wu Y, Yang Z, Liang X, Lei Z, Huang H, et al. Formation structure and properties of biocompatible TiZrHfNbTa high-entropy alloys. Mater Res Lett. 2019;7:225-31. http://dx.doi.org/10.1080/21663831.2019.1584592.

2. Geetha M, Singh AK, Asokamani R, Gogia AK. Ti based biomaterials, the ultimate choice for orthopaedic implants: a review. Prog Mater Sci. 2009;54:397-425. http://dx.doi.org/10.1016/j.pmatsci.2008.06.004.

3. Aksakal B, Yildirim OS, Gul H. Metallurgical failure analysisof various implant materials used in orthopedic applications. J Fail Anal Prev. 2004;4:17-23. http://dx.doi.org/10.1007/s11668-996-0007-9.

4. Liang S. Review of the design of titanium alloys with low elastic modulus as implant materials. Adv Eng Mater. 2020;22:2000555. http://dx.doi.org/10.1002/adem.202000555.

5. Okulov IV, Okulov AV, Soldatov IV, Luthringer B, Willumeit-Romer R, Wada T, et al. Open porous dealloying-based biomaterials as a novel biomaterial platform. Mater Sci Eng C. 2018;88:95-103. http://dx.doi.org/10.1016/j.msec.2018.03.008.

6. Luthringer BJ, Ali F, Akaichi H, Feyerabend F, Ebel T, Willumeit R. Production, characterisation, and cytocompatibility of porous titanium-based particulate scaffolds. J Mater Sci Mater Med. 2013;24:2337-58. http://dx.doi.org/10.1007/s10856-013-4989-z.

7. Prashanth K, Zhuravleva K, Okulov I, Calin M, Eckert J, Gebert A. Mechanical and corrosion behavior of new generation Ti-45Nb porous alloys implant devices. Technologies. 2016;4:33. http://dx.doi.org/10.3390/technologies4040033.

8. Okulov IV, Weissmuller J, Markmann J. Dealloying-based interpenetrating-phase nanocomposites matching the elastic behavior of human bone. Sci Rep. 2017;7:20. http://dx.doi.org/10.1038/s41598-017-00048-4.

9. Li Y, Chao Y, Haidong Z, Shengguan Q, Li X, Li Y. New developments of Ti-based alloys for biomedical applications. Materials. 2014;3:1709-800. http://dx.doi.org/10.3390/ma7031709.

10. Miracle DB, Senkov ON. A critical review of high entropy alloys and related concepts. Acta Mater. 2017;122:448-511. http://dx.doi.org/10.1016/j.actamat.2016.08.081.

11. George EP, Raabe D, Ritchie RO. High-entropy alloys. Nat Rev Mater. 2019;4:515-34. http://dx.doi.org/10.1038/s41578-019-0121-4.

12. Castro D, Jaeger P, Baptista AC, Oliveira JP. An overview of high-entropy alloys as biomaterials. Metals. 2021;11:648. http://dx.doi.org/10.3390/met11040648.

13. Nagase T, Iijima Y, Matsugaki A, Ameyama K, Nakano T. Design and fabrication of Ti–Zr-Hf-Cr–Mo and Ti–Zr-Hf-Co-Cr–Mo high-entropy alloys as metallic biomaterials. Mater Sci Eng C. 2020;107:110322. http://dx.doi.org/10.1016/j.msec.2019.110322.

14. Ning C, Ding D, Dai K, Zhai W, Chen L. The effect of Zr content on the microstructure, mechanical properties and cell attachment of Ti–35Nb–xZr alloys. Biomed Mater. 2010;5:045006. http://dx.doi.org/10.1088/1748-6041/5/4/045006.

15. Zhang J, Sun F, Hao Y, Gozdecki N, Lebrun E, Vermaut P, et al. Influence of equiatomic Zr/Nb substitution on superelastic behavior of Ti–Nb–Zr alloy. Mater Sci Eng A. 2013;563:78-85. http://dx.doi.org/10.1016/j.msea.2012.11.045.

16. Banerjee R, Nag S, Stechschulte J, Freaer HL. Strengthening mechanisms in Ti-Nb-Zr-Ta and Ti-Mo-Zr-Fe orthopaedic alloys. Biomaterials. 2004;25:3413-9. http://dx.doi.org/10.1016/j.biomaterials.2003.10.041.

17. Mazigi O, Mathan BK, Xu J, Choe HC, Ye QS. Biocompatibility and biodegradation of a low elastic modulus Ti-35Nb-3Zr alloy: nanosurface engineering for enhanced biodegradation resistance. ACS Biomater Sci Eng. 2017;3:509-17. http://dx.doi.org/10.1021/acsbiomaterials.6b00563.

18. Gibson LJ, Ashby MF. Cellular solids: structure and properties. Cambridge: Cambridge University Press; 1999.

19. Sose S, Roy M, Bandyopadhyay A. Recent advances in bone tissue engineering scaffolds. Trends Biotechnol. 2012;30:546-54. http://dx.doi.org/10.1016/j.tibtech.2012.07.005.

20. Wei X, Zhuo L, Xin L, Jingjing T, Gang C, Bowen L, et al. Porous Ti-10Mo alloy fabricated by powder metallurgy for promoting bone regeneration. Sci China Mater. 2019;62:1053-64. http://dx.doi.org/10.1007/s40843-018-9394-9.

21. Wang CL, Chen HJ, Zhu XD, Xiao ZW, Zhang K, Zhang XD. An improved polymeric sponge replication method forbiomedical porous titanium scaffolds. Mater Sci Eng C. 2017;70:1192-9. http://dx.doi.org/10.1016/j.msec.2016.03.037.

22. Chen SY, Huang JC, Pan CT, Lin CH, Yang TL, Huang YS, et al. Microstructure and mechanical properties of open-cell porous Ti-6Al-4V fabricated by selective laser melting. J Alloys Compd. 2017;713:248-54. http://dx.doi.org/10.1016/j.jallcom.2017.04.190.

23. Heywood M, Shi Z, Li Y, Wen C, Kanwar J, Xiao Y, et al. Corrosion of porous Ti35Zr28Nb in Hanks' solution and 3.5wt.% NaCl. Mater Corros. 2019;70:529-36. http://dx.doi.org/10.1002/maco.201810423.

24. Chen YH, Frith JE, Dehghanmanshadi A, Attar H, Kent D, Soro NDM, et al. Mechanical properties and biocompatibility of porous titanium scaffolds for bone tissue. J Mech Behav Biomed Mater. 2017;75:169-74. http://dx.doi.org/10.1016/j.jmbbm.2017.07.015.

25. Torres-Sanchez C, Mushref FRA, Norrito M, Yendall K, Liu Y, Conway PP. The effect of pore size and porosity on mechanical properties and biological response of porous titanium scaffolds.

Microstructural Characterization and Wear Behavior of Porous Equimolar TiNbZr Medium-Entropy Alloys
Scaffolds Produced by Mechanical Alloying

7

Mater Sci Eng C. 2017;77:219-28. http://dx.doi.org/10.1016/j.msec.2017.03.249.

26. Lee CM, Ju CP, Chern Lin JH. Structure-property relationship of cast Ti-Nb alloys. J Oral Rehabil. 2002;29:314-22. http://dx.doi.org/10.1046/j.1365-2842.2002.00825.x.

27. Qingquan K, Xin L, Xuguang A, Wei F, Chao L, Jiang W, et al. Characterization and corrosion behaviour of Ti-13Nb-13Zr alloy prepared by mechanical alloying and spark plasma sintering. Mater Today Commun. 2020;23:101130. http://dx.doi.org/10.1016/j.mtcomm.2020.101130.

28. Wu J, Tan X, An X, Zhang J, Guo Y, Liu J, et al. Development of biomedical Ti-Nb-Zr-Mn alloys with enhanced mechanical properties and corrosion resistance. Mater Today Commun. 2022;30:103027. http://dx.doi.org/10.1016/j.mtcomm.2021.103027.

29. Henriques VAR, Oliveira JL, Diniz EF, Camargo EN, Luz TR. Production of Ti-22Nb-6Zr shape memory alloy by powder metallurgy. SAE Tech Pap. 2012;36:0467. https://doi.org/10.4271/2012-36-0467.

30. Wang X, Li Y, Xiong J, Hodgson PD, Wen C. Porous TiNbZr alloy scaffolds for biomedical applications. Acta Biomater. 2009;5:3616-24. http://dx.doi.org/10.1016/j.actbio.2009.06.002.

31. Krishna BV, Bose S, Bandyopadhyay A. Low stiffness porous Ti structures for load-bearing implants. Acta Biomater. 2007;3:997-1006. http://dx.doi.org/10.1016/j.actbio.2007.03.008.

32. Kumar RP, Girisha L, Pravinprabu T, Sahayaraj AF, Kumar SNSS, Subbiah R. Analysis of abrasive wear resistance on scandium composite. Mater Today Proc. 2021. In press. http://dx.doi.org/10.1016/j.matpr.2021.01.203.

33. Rajkumara M, Kannan NS, Bruhathi M, Malteshkumar L, Girisha L, Sahayaraj AF, et al. Cryogenic treatment and taguchi optimization of Haynes alloy. Mater Today Proc. 2022;51:666-9. http://dx.doi.org/10.1016/j.matpr.2021.06.159.

34. Zhang L, Qu X-H, Duan B-H, He X-B, Qin M-L. Effect of porosity on wear resistance of SiCp/Cu composites prepared by pressureless infiltration. Trans Nonferrous Met Soc China. 2008;18(5):1076-82. http://dx.doi.org/10.1016/s1003-6326(08)60184-3.